Maximum Shortening Velocity and Power Are Reduced in a Human Cross-bridge Model of Type 2 Diabetes

Julia H Musgrave[1], June-Chiew Han[1], Marie-Louise Ward[1], Andrew J Taberner[1], Kenneth Tran[1]

[1] University of Auckland, Auckland, New Zealand

Abstract

Human cardiac trabeculae were studied to identify the effects of diabetes on passive and active tissue mechanical properties. The sensitivity of cross-bridge cycling kinetics to [ATP] and [P_i] was probed using small-amplitude sinusoidal perturbations in a custom-built device. The diabetic muscles produced lower active and passive stresses, and the complex modulus data revealed that they also had slower cross-bridge cycling kinetics. These data were used to parameterise metabolite-sensitive cross-bridge models representing diabetic and non-diabetic cohorts. These cross-bridge models were then integrated within a muscle model to simulate twitch dynamics and stress-length work-loops. The diabetic model had slower twitch kinetics reduced maximum shortening velocity and reduced muscle shortening power. Simulation of changes in metabolic state revealed that, while increasing [P_i] reduced muscle shortening power in both groups, the reduction was less pronounced in the diabetic model. These results suggest the presence of a compensatory mechanism to mitigate the effects of metabolic dysfunction in the diabetic heart.

1. Introduction

Type 2 diabetes is a highly complex and increasingly prevalent disease which often leads to diabetic cardiomyopathy, where diabetes causes negative effects on the functional properties of the heart and its tissues. Diabetes is known to cause mitochondrial dysfunction [1] at the cell level and impair myocardial force generation at the organ level [2]. However, the mechanisms of disease, and the interaction between mechanical and energetic effects on work and power output, remain unclear.

Our previous work has validated methods for parameterising cross-bridge models using active complex modulus data from permeabilised cardiac tissues [3]. We have recently presented extensive methods to develop and parameterise cross-bridge models to be responsive to changes in cellular metabolic state by incorporating dependencies on [ATP] and [P_i] [4]. Here we present the first instance of extending this work to human cardiac tissues. We have measured cardiac cross-bridge kinetics under different metabolic conditions in human cardiac tissues from diabetic and non-diabetic patients. We then parameterised our cross-bridge models with these data, integrated these models within a muscle model, and performed work-loop simulations to predict how diabetes affects cardiac work, shortening velocity and power output.

2. Methods

2.1. Measuring mechanical properties

Cardiac trabeculae (10 from patients with type 2 diabetes and 10 from patients without diabetes) were dissected from right atrial appendage samples donated by consenting patients undergoing coronary artery bypass surgery at Auckland City Hospital (approval HDEC 17/STH/61). Measurements were performed using our custom-built experimental device [5, 6], following protocols described in [4]. Briefly, dissected trabeculae were placed in 4 °C permeabilisation solution for ∼20 h. Permeabilised muscles were washed thoroughly in relaxing solution (pH 7.0, pCa 9.0, 7 mM EGTA, 20 mM imidazole, 5 mM MgATP, 1 mM P_i, 1 mM Mg^{2+}, 14.5 mM CrP, 180 mM ionic strength), before being mounted in the device and gradually stretched to an optimal sarcomere length of 2.2 μm. Muscle diameters were measured to allow the conversion from tensile force to stress. Experiments were performed at 37 °C.

The passive properties of each muscle were measured first. The force-length relationship was found by measuring passive stress at 85 %, 90 %, 95 % and 100 % of optimal muscle length. The passive complex modulus was also measured to quantify visco-elastic behaviour.

Measurements made in full calcium activation (pCa 4.5) were taken under five different metabolic conditions of varying [MgATP] and [P_i] (Table 1). These were applied to the muscles based on a balanced Latin square design to account for any effects arising from order of presentation. Trabeculae were first immersed in pre-activating solution [4] for 60 s, before switching to a bath of activating so-

lution (relaxing solution with pCa 4.5, 240 U/mL creatine kinase and the relevant concentration of MgATP and P_i). In each activating solution, the maximum stress and total complex modulus were recorded at steady state.

Complex modulus measurements were taken across 12 frequencies between 0.1 Hz and 100 Hz, with length perturbations of 0.25 % of the optimal muscle length. The active complex modulus was found by subtracting the passive complex modulus from each of the total complex moduli [3].

2.2. Model development

The averaged active complex moduli and steady-state stresses across the five different metabolite concentrations were used to parameterise our cross-bridge model for both diabetic and non-diabetic trabeculae. As in our previous work [4], the linearised version of the model was used to optimise the model parameters for a range of different metabolite and strain dependencies. The model permutation which produced the best fit for both sets of data incorporated ATP dependence using rapid equilibrium (between states C^1 and C^2), direct P_i dependence (at k_{-1}), and had strain dependencies on the cross-bridge binding rate and the cross-bridge detachment rate (Figure 1). Active stress produced by the model is given by:

$$F_a = K(Bx_B + Cx_C), \quad (1)$$

where K is a stiffness coefficient encompassing the density and individual stiffness of cross-bridges, B and C are state proportions, and x_B and x_C are mean cross-bridge strains. The 12 optimal parameters for the cross-bridge models (non-diabetic, diabetic) were as follows:

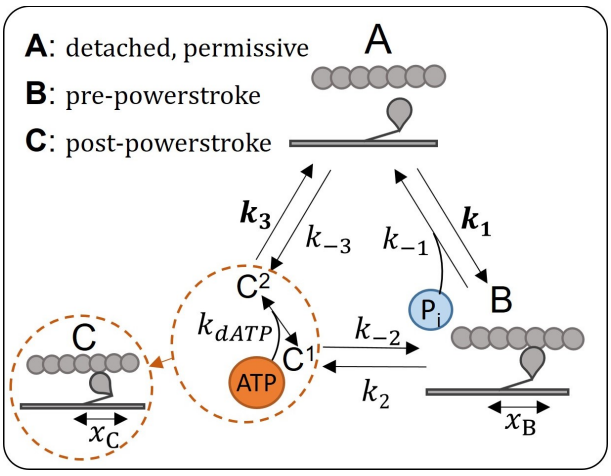

Figure 1. Schematic of the cross-bridge model that was parameterised to our experimental data from human trabeculae. The cycling rates in bold (k_1 and k_3) depend on cross-bridge strain.

k_1= (64, 39), k_{-1}= (2.5, 0.6), k_2=(41, 17), k_{-2}= (200, 98), k_3= (185, 93), ϕ_x= (2, 4.5), ϕ_v= (0.013, 0.012), ϕ_l= (5, 5), K= (24000, 16700), ϕ_{s1}= (606, 1), ϕ_{s3}= (206, 751), k_{dATP}= (0.18, 5).

A simple passive model was also fitted to the experimental data and combined with the cross-bridge model to create a muscle model. The passive complex modulus was used to capture the visco-elastic parameters at optimal length, as in [3]. An exponential equation for the purely elastic element was used to better fit the non-linearity of the passive force-length relationship.

As our cross-bridge model and data describe only the fully activated muscle state, we coupled it to the thin filament Ca^{2+} activation component of the Land et al. (2017) human model [7]. This introduced a non-permissive cross-bridge state and troponin binding kinetics to allow simulation of stress production under transient changes in intracellular Ca^{2+} concentration. The thin filament parameters and the Ca^{2+} transient used to drive the model were taken from [7]. The full muscle model consists of a cross-bridge component, a passive force component and a thin filament Ca^{2+} activation component.

2.3. Model simulations

Simulations were conducted using the full muscle model to predict how differences in cross-bridge kinetics induced by diabetes affected muscle mechanics under loading conditions similar to those experienced by the *in vivo* heart. Cardiac stress-length work-loops were simulated as a one-dimensional analogue to the three-dimensional pressure-volume loop. Following the protocol described in [8], prescribed afterloads range from the passive stress of the muscle to the maximum stress produced in an isometric twitch. In the first phase of a work-loop, the muscle contracts isometrically until it produces enough stress to overcome the prescribed afterload; this is followed by an isotonic contraction where the muscle shortens to maintain the afterload. In the third phase, the muscle relaxes isometrically once the stress falls below the afterload (end-systolic point), before being gradually re-stretched back to the initial length in the final phase.

The work done during a given work-loop was found by integrating the stress with respect to sarcomere length. We also quantified the extent of shortening throughout the loop and the maximum velocity of shortening. This latter metric allowed for the calculation of maximum power of shortening, by multiplying the maximum velocity by the given afterload. The simulations were initially performed using the baseline metabolite conditions of 5 mM MgATP and 1 mM P_i. To predict the effects of metabolic dysfunction, we also simulated work-loops at a higher [P_i] of 10 mM. All simulations were performed using MATLAB.

3. Results

3.1. Trabecula mechanics

The steady-state stresses developed by diabetic trabeculae under full Ca^{2+} activation were lower than those developed by non-diabetic trabeculae across the metabolite conditions studied (Table 1; two-way ANOVA group effect, $p < 0.05$). The passive stress was also lower in the diabetic group (t-test, $p < 0.05$).

Table 1. Active and passive steady-state stress values (mean ± SE) across the two groups. The top row represents baseline metabolic conditions.

[ATP] (mM)	[P_i] (mM)	Non-diabetic stress (kPa)	Diabetic stress (kPa)
5	1	20.4 ± 1.8	16.2 ± 2.1
0.1	1	24.9 ± 2.8	18.9 ± 2.3
1	1	21.5 ±2.7	19.0 ± 3.1
5	0	20.9 ± 2.4	17.1 ± 2.2
5	10	17.0 ± 1.6	12.6 ± 1.8
Passive stress		4.8 ± 0.5	3.4 ± 0.4

These results were reflected in the complex modulus measurements, where the diabetic active complex moduli had lower magnitudes than those of the non-diabetic group (Figure 2 shows data for baseline conditions; two-way ANOVA group effect, $p < 0.05$). There was also a subtle leftward shift in the active complex moduli of the diabetic group, indicating slower cross-bridge cycling rates. The typical effects of higher stiffness and leftward shifts with decreasing ATP or P_i (and vice versa) were present in the averaged experimental data for both groups.

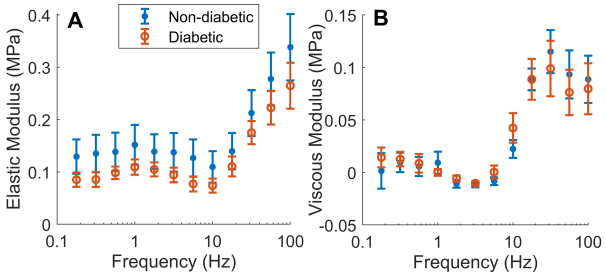

Figure 2. Active complex modulus (mean ± SE) at baseline conditions (5 mM ATP and 1 mM P_i).

3.2. Work-loop simulations

Figure 3A shows a series of work-loops simulated in the non-diabetic and diabetic muscle models for the lowest, highest and two intermediate afterloads. Figure 3B shows the stress profile over time for each of these simulations. The isometric twitch, which is equivalent to the work-loop with the maximum afterload, is bolded and clearly shows a lower peak stress reached by the diabetic model (19.2 kPa vs 15.7 kPa), as well as slower twitch dynamics (duration of twitch above 5% of peak stress of 677 ms vs 441 ms).

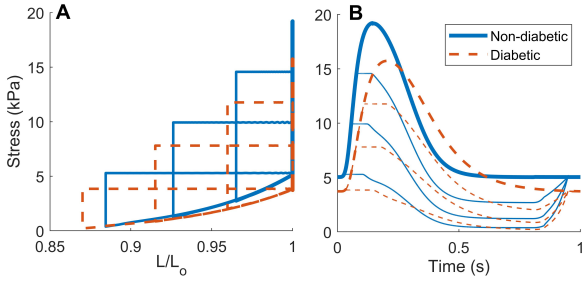

Figure 3. Effect of diabetes on simulated (A) stress-length work-loops and (B) stress profile; isometric twitch in bold.

Analysis of work-loops simulated by the two muscle models showed that the work produced at a given relative afterload was slightly lower in diabetes (Figure 4A). While the extents of shortening were also similar, those of the diabetic model were slightly greater (Figure 4B). The most pronounced effect of diabetes was on reducing the maximum shortening velocity and power of shortening of work-loops at all relative afterloads (Figure 4C & D).

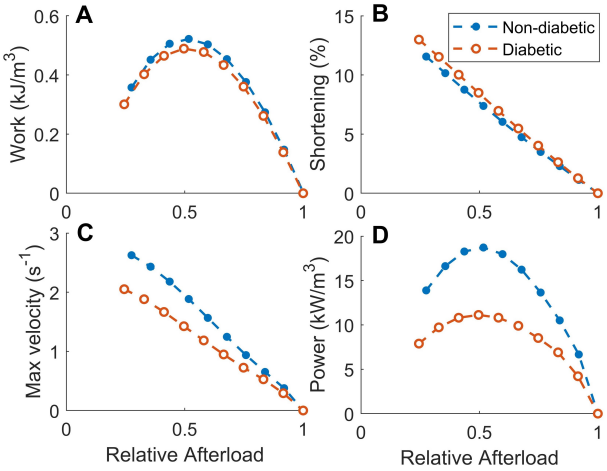

Figure 4. Simulations of work (A), extent of shortening (B), maximum shortening velocity (C) and maximum power of shortening (D) under baseline metabolic conditions.

Work-loops were also simulated under different concentrations of P_i. As expected, an increase in [P_i] caused a decrease in stress development and consequently lower work, shortening and power (Figure 5). However, in the diabetic group, the reduction in work and power was less pronounced, suggesting a lower sensitivity to P_i in diabetes.

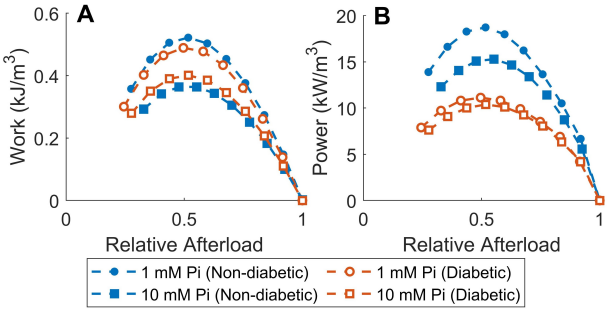

Figure 5. Simulations of work (A) and maximum power of shortening (B) at low and high concentrations of P_i.

4. Discussion

We have measured cross-bridge properties in human cardiac trabeculae from diabetic and non-diabetic patients. Using these data, we constructed a full muscle model for simulating work-loop contractions. Our simulations revealed that diabetes reduces maximum twitch force and slows muscle twitch kinetics (Figure 3) which ultimately results in a reduction in cardiac shortening velocity and power output (Figure 4). The key disease mechanism driving these phenotypes appears to be a diabetes-induced reduction in a majority of cross-bridge cycling rates. Our model parameterisation also produced a lower value of K (Eq. 1) in the diabetic model, which is consistent with either reduced cross-bridge stiffness or density.

Driven by a lower value of k_{-1}, the diabetic model had a decreased sensitivity to P_i, which was reflected in work-loop simulations (Figure 5). As diabetic hearts are known to have an increased P_i/PCr ratio [9], this provides evidence for a compensatory mechanism in the diabetic heart to mitigate further reductions of power output under perturbed metabolic conditions where $[P_i]$ is elevated. The measurement of lower passive stress in the diabetic group was unexpected as diastolic dysfunction is one of the early symptoms of diabetic cardiomyopathy [2]. However this is not inconsistent with findings from a study of intact trabeculae from a similar patient cohort, which found no differences in the diastolic stress, despite significantly increased diastolic Ca^{2+} in diabetes [10]. We have additionally confirmed that the key findings of our study are independent of the passive force model and thus reflect the active properties measured in our experiments.

While there are reported effects of diabetes on Ca^{2+} dynamics [10], we have chosen to drive work-loops for both diabetic and non-diabetic models using the same Ca^{2+} transient. In doing so, we have isolated, and revealed, the effects of diabetes specifically on cardiac cross-bridge function.

Acknowledgements

We thank Auckland City Hospital staff and patients for their generous donation of cardiac tissues, and Paige Karanikolaou for assistance with tissue collections. This research was funded by a UoA Doctoral Scholarship (JM), Sir Charles Hercus Fellowships (20/011 and 21/116) from the Health Research Council of NZ (J-CH and KT) and an Auckland Medical Research Foundation Project Grant (1121010, M-LW).

References

[1] Bugger H, Abel ED. Mitochondria in the diabetic heart. Cardiovasc Res Nov. 2010;88(2):229–240.

[2] Tan Y, Zhang Z, Zheng C, Wintergerst KA, Keller BB, Cai L. Mechanisms of diabetic cardiomyopathy and potential therapeutic strategies: preclinical and clinical evidence. Nat Rev Cardiol 2020 179 Feb. 2020;17(9):585–607.

[3] Musgrave JH, Han JC, Ward ML, Taberner AJ, Loiselle DS, Tran K. Uncovering cross-bridge properties that underlie the cardiac active complex modulus using model linearisation techniques. Math Biosci Nov. 2022;353:108922.

[4] Musgrave JH, Han JC, Ward ML, Taberner AJ, Tran K. Analysis of metabolite and strain effects on cardiac cross-bridge dynamics using model linearisation techniques. Front Physiol Jan. 2024;14.

[5] Choi DH, Pham T, Loiselle DS, Taberner AJ, Han JC, Tran K. The Inverse Relationship between Cardiac Muscle Stress and Cross-Sectional Area Is Preserved in Ba2+ Contracture and in Chemically-Permeabilised Ca2+ Contracture. Exp Mech Jan. 2021;61(1):107–117.

[6] Musgrave JH, Han JC, Ward ML, Taberner AJ, Tran K. Measuring and Modelling the Effect of Inorganic Phosphate on Cross-bridge Mechanics in Human Cardiac Muscle. In 45th Annu. Int. Conf. IEEE Eng. Med. Biol. Soc. 2023; .

[7] Land S, Park-Holohan SJ, Smith NP, dos Remedios CG, Kentish JC, Niederer SA. A model of cardiac contraction based on novel measurements of tension development in human cardiomyocytes. J Mol Cell Cardiol Apr. 2017;106:68–83.

[8] Tran K, Han JC, Crampin EJ, Taberner AJ, Loiselle DS. Experimental and modelling evidence of shortening heat in cardiac muscle. J Physiol Oct. 2017;595(19):6313–6326.

[9] Valkovič L, Apps A, Ellis J, Neubauer S, Tyler DJ, Schmid AI, Rider OJ, Rodgers CT. Increased cardiac Pi/PCr in the diabetic heart observed using phosphorus magnetic resonance spectroscopy at 7T. PLoS One Jun. 2022;17(6):e0269957.

[10] Jones TLM, Kaur S, Kang N, Ruygrok PN, Ward ML. Impaired calcium handling mechanisms in atrial trabeculae of diabetic patients. Physiol Rep Jan. 2023;11(3).

Address for correspondence:

Julia Musgrave
70 Symonds Street, Grafton, Auckland 1010, New Zealand
julia.musgrave@auckland.ac.nz